NanoImpact 28 (2022) 100424

Contents lists available at ScienceDirect

NanoImpact

journal homepage: www.elsevier.com/locate/nanoimpact

# Metal doped nitrogenous hydroxyapatite nanohybrids slowly release nitrogen to crops and mitigate ammonia volatilization: An impact assessment

Bhaskar Sharma [a,b], Manoj Shrivastava [d], Luis O.B. Afonso [a], Udit Soni [c,*], David M. Cahill [a,*]

[a] School of Life and Environmental Sciences, Deakin University, Geelong Waurn Ponds Campus, Geelong, VIC 3216, Australia
[b] Department of Botany and Plant Sciences, University of California-Riverside, Riverside, CA 92521, United States
[c] Department of Biotechnology, TERI School of Advanced Studies, New Delhi 110070, India
[d] ICAR-Indian Agricultural Research Institute, Pusa, New Delhi 110012, India

ARTICLE INFO

Editor Name: Dr. Bernd Nowack

*Keywords:*
Slow-release nitrogen fertilizer
Zinc and magnesium doped hydroxyapatite-urea nanohybrids
Ammonia emissions mitigation
Sustainable environment
Impact assessment

ABSTRACT

To supply adequate food, the ongoing and unrestrained administration of nitrogen fertilizer to agricultural fields is polluting the climate and living organisms. On the other hand, the agriculture sector urgently needs a technological upgrade to effectively confront hunger and poverty. Here, we report a rapid synthesis of zinc and magnesium-doped hydroxyapatite-urea nanohybrids for slow release and delivery of nitrogen to wheat and rice crops. Nanohybrids slowly release nitrogen for up to six weeks compared to the burst release of nitrogen from urea, and their use substantially reduces, by at least 3.8 times, ammonia emissions into the environment compared with that of urea fertilizer. A half-nitrogen dose applied as multi-nutrient complexed nanohybrids maintained crop growth, yield, and nutritional compositions in wheat and subsequent rice crops. Nanohybrids enhanced the wheat crop yield and nitrogen uptake by 22.13% and 58.30%, respectively. The synthesized nitrogen nanohybrids remained in the soil for two continuous crop cycles, reduced ammonia volatilization, and achieved nitrogen delivery to the crops. Additionally, soil dehydrogenase activity (534.55% above control) and urease activities (81.82% above control) suggest that nanohybrids exhibited no adverse impact on soil microorganisms. Our comprehensive study demonstrates the advantages of 'doping' as a method for tailoring hydroxyapatite nanoparticles properties for extended agricultural and environmental applications. The use of nanohybrids substantially reduced greenhouse gas emissions and enabled the reduction, by half, of nitrogen inputs into the agricultural fields. This study, therefore, reports a novel nano-enabled platform of engineered hydroxyapatite-urea nanohybrids as a nitrogen fertilizer for efficient nitrogen delivery that results in improved crop growth while minimizing environmental pollution.

## 1. Introduction

As the world's population will approach 9.73 billion by 2050, global food demand is expected to rise by 100–110% (Tilman et al., 2011; van Dijk et al., 2021; Alexandratos and Bruinsma, 2012). Most developing countries will need to boost agricultural output to feed their population. However, the consequent excess use of chemical fertilizers causes severe damage to the environment, including impacts on soil friability, holding capacity, pH and nutrient content, microbial biomass, and causes aquatic resource contamination (Good and Beatty, 2011; Raimbault and Vyn, 1991; Hussain et al., 1988).

In the soil environment, nitrogen fertilizers are either directly absorbed by plants or converted into other forms by oxidation processes (Reddy et al., 1984; Cameron et al., 2013). Therefore, a high amount of nitrogen fertilizer is applied to the soil, to account for losses such as leaching and volatilization, to meet optimum plant growth requirements (Huang and Uri, 1993). Nitrogen fertilizer overabundance in farmlands leads to several broad-scale environmental problems, such as the greenhouse effect, acid rain, and eutrophication, and may directly impact human health (Gastal and Lemaire, 2002; Wang et al., 2002; Ikemoto et al., 2002). In particular, nitrate and nitrous oxide release from agricultural systems has been recognized as a threat to both the

* Corresponding authors.
*E-mail addresses:* bhaskar.sharma@research.deakin.edu.au, bsharma@ucr.edu (B. Sharma), luis.afonso@deakin.edu.au (L.O.B. Afonso), uditsoni.iitd@gmail.com (U. Soni), david.cahill@deakin.edu.au (D.M. Cahill).

https://doi.org/10.1016/j.impact.2022.100424
Received 17 May 2022; Received in revised form 30 August 2022; Accepted 31 August 2022
Available online 7 September 2022

environment and human health (Tilman et al., 2002; Setty et al., 2017).

Approximately two-thirds of the total nitrogen fertilizer applied accumulates in the soil, and at least one-fifth of the accumulated nitrate leaches into groundwater (Yadav, 1997). High nitrogen application is directly proportional to the level of nitrate accumulation in the soil (Lu et al., 2019). Global ammonia emission has increased 8.7 times from 1.9 ± 0.03 to 16.7 ± 0.5 Tg N per year between 1961 to 2010 because of excessive nitrogen fertilizer use (Xu et al., 2019). Crops of rice, wheat, and corn have been the major contributor to global ammonia emissions for the last three decades (Xu et al., 2019). The immediate solution can be either to reduce the amount of chemical fertilizer application in the field or to use safer alternatives to chemical fertilizers.

Slow-release fertilizers are attractive alternatives to conventional fast-release chemical fertilizers by showing a controlled release pattern over time and remaining longer in the soil (Trenkel, 1997; Dimkpa et al., 2020). Nanomaterials, due to their unique properties such as high surface area, smaller size and shape, have become suitable candidates for the delivery of nutrients (Jampílek and Kráľová, 2017; Gilbertson et al., 2020). Nanomaterials have the potential to reduce chemical fertilizer input while maintaining or boosting agricultural output (Hofmann et al., 2020; Avellan et al., 2021). Layered double hydroxide, chitosan, zeolite, and nano-urea have been reported to slowly release the nutrients (Aziz et al., 2016; Dubey and Mailapalli, 2019; Bansiwal et al., 2006; Songkhum et al., 2018). However, the agriculture sector still needs more robust and feasible technologies to establish nanomaterials as a new medium of nutrient delivery. Hydroxyapatite has recently been shown to hold nitrogen through weak interactions and slowly release nitrogen into the soil, improving crop growth (Sharma et al., 2022a).

Hydroxyapatite is a crystalline, thermostable, and biodegradable mineral augmented with calcium and phosphorus, which is used widely in bone tissue engineering and dental repairs (Tao et al., 2007; Dinarvand et al., 2011). Nanoscale-sized hydroxyapatite has also been investigated as a source of phosphorus fertilizer (Liu and Lal, 2014). One study, for example, found that nano-hydroxyapatite loaded with phosphorus was taken up by root epidermal cells and then travelled into the cortical apoplast, where the more acidic environment dissociated the phosphorus from the nano-hydroxyapatite providing phosphorus to phosphorus-deficient plants (Szameitat et al., 2021).

In our previous reports, we demonstrated that the surface area of the hydroxyapatite could be improved by modulating the size and shape of the particles through doping with metal ions (Sharma et al., 2022b; Sharma et al., 2022a). In the present study, zinc and magnesium doped and undoped hydroxyapatite nanoparticles that we term 'nanohybrids' were synthesized and modified to carry nitrogen as urea on their surfaces. Plant nutrients supplied this way could include beneficial elements such as calcium, phosphorus, zinc, and magnesium. We showed that the doped hydroxyapatite-urea slowly released nitrogen for one week, improving the wheat crop growth and soil available nitrogen. This study further explored the ammoniacal-N and nitrate-N release dynamics from doped hydroxyapatite-urea in the soil under controlled and field environment conditions, as they are critical for crop growth and environment. The nanohybrid materials were further assessed for their impact on ammonia volatilization, soil microbial activities, nutrient uptake and growth in wheat and rice crops.

## 2. Material and methods

### 2.1. Nanohybrids synthesis

The method of synthesis of the nanohybrids followed that of Sharma et al. (2022a). Briefly, 1 M calcium hydroxide suspension was stirred at 450 rpm for 30 min, and 0.6 M ortho-phosphoric acid was added dropwise to the solution. The resulting mixture was stirred for three hours at 50 °C and dried at 65 °C to obtain hydroxyapatite nanoparticles. The hydroxyapatite nanoparticles were then doped using 0.05 M magnesium chloride hexahydrate and 0.05 M zinc sulfate heptahydrate, respectively, with 0.95 M calcium hydroxide to produce magnesium-doped and zinc-doped hydroxyapatite nanoparticles.

For the preparation of hydroxyapatite-urea, the method of Sharma et al. (2022a) was followed whereby 7 M urea and 1 M calcium hydroxide suspension was stirred at 450 rpm for 45 min. Then 0.6 M ortho-phosphoric acid was added dropwise to the solution with continuous stirring at 450 rpm for three hours at 50 °C. Similarly, 7 M urea was used separately with 0.95 M calcium hydroxide and 0.05 M magnesium chloride hexahydrate for magnesium-doped hydroxyapatite-urea, and 0.95 M calcium hydroxide and 0.05 M zinc sulfate heptahydrate for zinc-doped hydroxyapatite-urea nanohybrids production and then stirred at 450 rpm for 45 min. Then 0.6 M ortho-phosphoric acid was added dropwise to the solution with continuous stirring at 450 rpm for three hours at 50 °C. The resulting slurry was dried at 65 °C, and the three varieties of nanohybrids were obtained: hydroxyapatite-urea, magnesium-doped hydroxyapatite-urea, and zinc-doped hydroxyapatite-urea. (Sharma et al., 2022a).

### 2.2. Material characterization

#### 2.2.1. Powder X-ray diffraction

Powder X-ray diffraction (PXRD) of the dried samples milled for fifteen minutes into a powder, and where no soller slit was used, was carried out on a Bruker D8 Advance diffractometer with a 2theta range of 10 to 60° used for sample analysis.

#### 2.2.2. Fourier transform infrared spectroscopy

The FTIR spectrum was obtained in the region 4000 to 400 $cm^{-1}$ using the KBr-disc method for sample preparation on a Varian 7000 FTIR instrument to evaluate the functional groups of the nanohybrids.

#### 2.2.3. Cryo-transmission electron microscopy

Transmission electron micrography of the samples was performed on a TALOS cryo transmission electron microscope at an accelerating voltage of 200 kV. Samples were dispersed in MiliQ water followed by sonication for 15 min and cast on carbon-coated copper grids (300 mesh) by dropping directly onto the grid and then incubated for one hour at room temperature.

#### 2.2.4. Scanning electron microscopy

Scanning electron microscope (SEM) images of the dried samples were acquired on a TESCAN LYRA3 SEM, a focused ion beam scanning electron microscope equipped with SE detectors (using an accelerating voltage of 20 kV). The dried sample powder was sprinkled on a black carbon tape surface on steel grids, and the samples were coated with ultrathin electrically conducting gold metal before imaging.

#### 2.2.5. Energy-dispersive X-ray analysis

Energy-dispersive X-ray analysis was performed for all the nanohybrids on the TESCAN instrument using a high-energy beam accelerating voltage of 15 kV.

#### 2.2.6. Hydrodynamic particle size and zeta potential

The average hydrodynamic diameter and zeta potential of the synthesized urea-nanohybrids and bare nanoparticles were determined using a Horiba Particle Analyzer SZ-100 V2 instrument.

### 2.3. Experimental field soil analysis

The experimental field soil was classified as Ustochrept in the order of Inceptisol. The texture of the experimental surface soil (0–15 cm) was sandy clay-loam soil (50.8% sand, 23.2% silt, and 25.9% clay), determined by the hydrometer method (Bouyoucos, 1962). Experimental soil had 225 kg $ha^{-1}$ alkaline permanganate oxidizable nitrogen (N) (Subhaiaih and Asija, 1956), 12.2 kg $ha^{-1}$ available phosphorus (P) (Olsen, 1954), 226 kg $ha^{-1}$ ammonium acetate exchangeable potassium (K)

(Hanway and Heidel, 1952) and 5.5 g $kg^{-1}$ organic carbon (C) (Walkley and Black, 1934) using previously reported methods. The pH of the soil was 7.9 (1:2.5 soil: water ratio) (Srivastava and Singh, 2009), and diethylene triamine penta acetic acid (DTPA)-extractable zinc (Lindsay and Norvell, 1978) in soil was 0.63 mg $kg^{-1}$ soil. Fifty kilograms of the surface soil from the experimental field were collected, passed through a 2 mm sieve, and used for the nitrogen release kinetics experiment.

### 2.4. Nitrogen release study

The granular urea and nanohybrids nitrogenous sources containing 200 mg nitrogen each were mixed with 1000 g of soil in two-litre volume beakers, and moisture in the soil was maintained at field capacity throughout the experiment by adding distilled water and incubating at 25 °C for 42 days. All treatments were kept in triplicate. The soil was collected at different intervals to analyse nitrate-N and ammonical-N release from nanohybrids in the soil. The ammoniacal-nitrogen and nitrate-nitrogen were estimated using KCl extraction followed by spectrophotometry (Fishman and Friedman, 1989), and total nitrogen was estimated using the Kjeldahl method (Nelson and Sommers, 2020). The total available nitrogen was evaluated through the Kjeldahl method using alkaline potassium permanganate as an oxidative agent (Subbaiah, 1956; Bremner, 1960).

### 2.5. Field experiments

The field experiment was conducted during the winter (wheat) and monsoon (rice) season at the research farm of the Indian Agricultural Research Institute, New Delhi, located at 28.08°N latitude and 77.12°E longitudes in central Delhi with an elevation of 228.61 m above sea level. For wheat, the recommended N dose of 150 kg N per hectare was supplied (Sapkota et al., 2020; Giller et al., 2004). The phosphorus and potassium were applied uniformly as single super phosphate (SSP-16% $P_2O_5$) (60 kg $P_2O_5$ per hectare) and muriate of potash (MOP-60% $K_2O$) (60 kg per hectare), respectively, as per recommendation in all treatments. The experiment was laid out using a randomized block design (RBD) containing eight treatments: i) No fertilizer, ii) Granular urea 100% $RD_{NPK}$ (100% of recommended N dose), iii) Hydroxyapatite-urea at either 50% or 100% $RD_N$ + 100% $RD_{PK}$ (at either 50% or 100% of recommended N dose), and then iv) Mg-doped or Zn-doped Hydroxyapatite-urea at either 50% or 100% $RD_N$ + 100% $RD_{PK}$ (at either 50% or 100% of recommended N dose). All treatments were replicated three times. The full dose of the phosphorus and potassium fertilizers was applied as a basal dose at the sowing time. All the nitrogen fertilizers were applied in two instalments, half of the dose at the time of sowing and the remaining half at the tillering.

#### 2.5.1. Wheat crop treatment and analysis

Wheat seeds of the variety Pusa HD 3086 were used in this study. All the above treatments were implemented in a research plot of 6 square meters (3 m × 2 m). The wheat crop was grown in the winter season (28th November 2019 to 25th April 2020). Soil sampling was performed at the time of harvesting to determine ammonical and nitrate nitrogen release and available nitrogen. The crop was maintained with regular irrigation and other standard agronomic practices. Plants were harvested at maturity. The plant height, number of effective tillers, spike length, 1000-grain weight, biomass yield, chlorophyll content, and leaf area index were recorded. Grain, straw, and root samples were dried at 70 °C after harvesting and processed for elemental (phosphorus, nitrogen, potassium, calcium, magnesium, zinc, iron, manganese) and grain quality analysis.

#### 2.5.2. Rice crop treatment and analysis

Rice crop cv. Pusa Basmati 1121 (PB 1121) was grown to examine the residual impact of the different nitrogenous fertilizers on crop growth, development, and productivity. Rice seeds were germinated separately by 17th June 2020 and then transplanted to the plots nine days after germination. The nano-fertilizer research plots were supplemented with a 50% dose of the total recommended nitrogen (60 kg N/ha), while control plots (Granular Urea) were supplemented with a 100% dose of total recommended nitrogen (120 kg N/ha) (Giller et al., 2004; Sapkota et al., 2020). The phosphorus and potassium were applied as SSP (60 kg $P_2O_5$ per hectare) and MOP (60 kg $K_2O$ per hectare), respectively. The full doses of phosphorus and potassium fertilizers were applied at the time of sowing. Each nitrogen fertilizer was applied in two instalments, half of the dose at the time of sowing and the remaining half at the tillering. Nine days old rice seedlings were transplanted per hill in the puddled field at a spacing of 20 cm × 15 cm. All plots were submerged by maintaining a 5–10 cm water level over the soil surface, up to the milk stage, by irrigation as and when required. The transplanting was performed on 27th June 2020, and the crop was harvested on 15th November 2020. Plant height, number of effective tillers, panicle length, number of grains in panicles, chlorophyll content, thousand kernel weight, biomass yield, and straw weight was recorded after crop harvesting. The grain, stem, and root tissues were processed for total nitrogen analysis and grain quality analysis.

### 2.6. Estimation of ammonia volatilization

Ammonia volatilization was estimated using the forced air draft method (Stumpe et al., 1984). A closed chamber made from 6 mm thick acrylic sheets measuring 20 cm × 20 cm × 50 cm (L*W*H) was placed in the treatment plots. The volatilized $NH_3$ gas from the soil surface under different treatments was collected in a 2% Boric acid solution containing mixed indicators (methyl red and bromocresol green). The gas inside the chamber was collected into boric acid traps using a vacuum pump having a flow rate of 3 L $min^{-1}$. The volatilized ammonia-nitrogen was determined by titration of the boric acid solution with 0.02 N sulphuric acid (Bremner, 1960). For the wheat crop treatments, ammonia volatilization was measured at the sowing and tillering stage (from 28th November to 28th December 2019), and for the rice crop, ammonia volatilization at the time of transplanting and tillering (27th June to 31st July 2020). Ammonia volatilization was measured twice daily during the period 7 am to 5 pm, and then again during the period 6 pm to 6 am (overnight). The amount of ammonia flux per unit area of soil was estimated using the following equation:

$$NH_3 \quad \text{volatilized} \quad \left(\mu g\ m^{-2} d^{-1}\right) = \frac{A \times 0.00028 \times 1000}{L \times W}$$

where A is the volume (mL) of sulphuric acid consumed and L and W are the length and width of the chamber (m) respectively.

### 2.7. Elemental and grain quality analysis

Total plant phosphorus was estimated by developing a stable yellow color using the phosphovanado-molybdate solution followed by spectrophotometric analysis (Hanson, W., 1950). Total calcium (Severenghaus and Ferrebee, 1950) and potassium (Brealey, 1951) were estimated using a flame photometer using calcium chloride and potassium dihydrogen phosphate as reference material. Magnesium was estimated using the EDTA titration method (Padhye, 1957). The concentration of zinc (Meret and Henkin, 1971), manganese (Zook et al., 1970), and iron (Zettner et al., 1966) were estimated using atomic absorption spectrophotometry. Total grain protein (Compton and Jones, 1985), phospholipid (Bahrami et al., 2014; Zilversmit and Davis, 1950), and proline content (Bates et al., 1973) were estimated for the assessment of grain quality.

### 2.8. Statistical analysis

Data for all parameters were analyzed statistically by analysing

variance (ANOVA). Means were compared for a significant difference where the analysis of variance was significant at '$p < 0.05$', '$p < 0.01$', '$p < 0.001$', and '$p < 0.0001$' using Dunnett's multiple comparison test.

## 3. Results and discussion

### 3.1. Characterization of Nano-hybrid nitrogenous fertilizers

The XRD pattern of hydroxyapatite nanoparticles revealed the polycrystalline nature of the nanoparticles (Fig. 1). The doping of the smaller ionic radius zinc (0.074 nm) and magnesium (0.072 nm) in hydroxyapatite replaced calcium ions (0.099 nm) that consequently modifying the hydroxyapatite structure. The reduced intensities, broadening of the peaks (211 and 002), and increased FWHM in doped hydroxyapatite suggested distortion of the crystallinity induced by bond strain and reduction in the size of the nanoparticles (Dasgupta et al., 2010; Sharma et al., 2022a). Crystal growth at the a-axis corresponding to the (200) plane and the c-axis corresponding to the (002) plane was expanded in the Zn and Mg-doped hydroxyapatite compared with that of the undoped HAP. The lattice expansion increased the surface area of nanoparticles, which could then accommodate more urea molecules on their surface. The crystalline size of the peak (211) was calculated to be 5.8 nm for MgHAP and ZnHAP compared to 7.26 nm for HAP.

Hydroxyapatite-urea showed a peak shift in the (111) and (210) planes compared to pure urea indicating weak interaction-mediated structural modifications. The XRD pattern of the Zn and Mg-doped hydroxyapatite-urea showed a distorted crystalline structure at the peak (211) with lower intensity. The crystalline size of the peak (211) was decreased to 11.22 nm in MgHAU and 11.51 nm in ZnHAU from 12.51 nm for the HAU. The interplanar spacing corresponding to (002) and (211) planes was 0.34 nm and 0.28 nm for all nanohybrids.

We observed urea molecule characteristic functional groups C—N (1460 $cm^{-1}$), N—H (1593 $cm^{-1}$ and 1595 $cm^{-1}$), and C═O (1678 $cm^{-1}$) and hydroxyapatite characteristic functional groups $PO_4^{3-}$ (1026 $cm^{-1}$ and 1092 $cm^{-1}$) and P—O (961 $cm^{-1}$) and O—P—O (563 $cm^{-1}$, 559 $cm^{-1}$, 602 $cm^{-1}$, 601 $cm^{-1}$) (Fig. 2) (Poinern et al., 2011; Sagle et al., 2009). The Zn and Mg-doped hydroxyapatite nanoparticles showed spectral shifts of $\upsilon_4$ vibrations of the O—P—O functional groups and $PO_4^{3-}$ compared with the undoped hydroxyapatite nanoparticles indicating a reorganized intermolecular bonding and structural modifications. Interestingly, the sharpest peaks were recorded for ZnHAP nanoparticles, but peak intensity was lost in ZnHAU nanohybrids after integrating with the urea molecules.

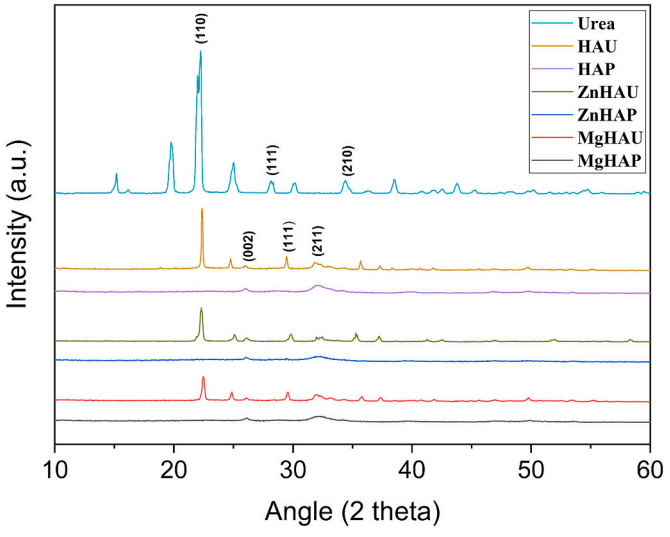


**Fig. 1.** Powder X-ray diffraction (PXRD) analysis of the synthesized nanohybrids (HAU, MgHAU, and ZnHAU), bare nanoparticles (HAP, MgHAP, and ZnHAP), and urea.

The shifts in the C═O and C—N regions of the ZnHAU, MgHAU and HAU could be attributed to a weak or unstable chemical environment induced by the changes in the dipole movement. The urea molecules could interact at the p site or negative site of the crystal through weak bonds (i.e., hydrogen bonds) that facilitated their surface adsorption. The sharpness of the O—P—O and $PO_4$ peaks declined, and peak broadening was noticed due to the changing chemical environment and the introduction of hydrogen bonding to the structure (Sharma et al., 2022a).

Following their synthesis, the initial, small bead-like structures grew into aggregates of crystalline, needle-shaped structured nanohybrids with a diameter of up to 100 nm (Fig. 3A–F). The HAU, MgHAU, and ZnHAU nanohybrids were transformed from rod-shaped into irregular round or rough hexagonal shaped and porous structures after adding urea molecules. The urea molecules bound to the surface of the rod-shaped HAP, MgHAP, and ZnHAP nanoparticles, and grew in various directions that changed the morphology of the nanohybrids (Fig. S1A–D).

The transmission electron micrograph of HAP showed a rod-shaped crystalline structure with a width of 13 nm and a length of 40 nm. The HAP nanostructures appeared as unorganized rods forming a spindle-like morphology resulting from a faster growth rate (Kumar et al., 2004). The average diameters of the urea-loaded HAU, MgHAU and ZnHAU were 71 nm, 54 nm, and 63 nm, respectively. Energy-dispersive X-ray analysis of the nanohybrids confirmed the presence of calcium, phosphorus, magnesium, zinc, and nitrogen elements (Fig. S2).

DLS measurements showed that the average particle size of the undoped hydroxyapatite nanoparticles was 356 ± 46.3 nm, which was reduced for both the magnesium- and zinc- doped hydroxyapatite nanoparticles to 167.8 ± 9.7 nm and 279.5 ± 26.1 nm, respectively (Fig. S3). The average hydrodynamic diameter of the urea-coated hydroxyapatite nanohybrids was 825.4 ± 91.6 nm, while magnesium and zinc doped hydroxyapatite-urea nanohybrids were found to be 466.8 ± 48.4 and 590.6 ± 51.6 nm, in diameter respectively. The hydroxyapatite nanoparticles appeared as aggregated rod-shaped structures and were therefore measured as relatively larger by DLS compared with that determined by TEM and XRD.

The Zeta potential of the hydroxyapatite, magnesium, and zinc-doped hydroxyapatite nanoparticles was 14.9 mV, 13.2 mV, and 4.3 mV, respectively. The zeta potential of the nanoparticles was altered to −2.7 mV, −11.1 mV, and − 2.4 mV in the hydroxyapatite-urea, magnesium-doped hydroxyapatite-urea, and zinc-doped hydroxyapatite-urea, respectively after urea coating. As has also been reported by Predoi et al. (2019), the zinc doping into hydroxyapatite decreased the zeta potential and induced rapid coagulation.

### 3.2. Nanohybrids slowly release nitrogen and mitigate ammonia volatilization

Ammoniacal and nitrate are preferable nitrogen forms for plant uptake (Yoon et al., 2020). The applied nitrogen fertilizers are transformed into ammoniacal-N and nitrate-N through chemical and enzymatic reactions in the soil (Hofman and Van Cleemput, 2004). Therefore, the ammoniacal-N and the nitrate-N release pattern from the synthesized nanohybrids in the soil environment can provide mechanistic insights into nitrogen mobilization into the crop and soil.

Approximately 22% of the total released ammoniacal-N and 9.1% of the total released nitrate-N were rapidly liberated from the urea molecules within 72 h of incubation in the soil (Fig. 4A–C). 26% ammoniacal-N and 13.2% nitrate-N was released from urea molecules within six days of soil incubation. All three forms of nanohybrids showed sustained release of ammoniacal and nitrate nitrogen. HAU nanohybrid released 1.7% ammoniacal-N and 5.4% nitrate-N compared with 4.6% and 4.9% ammoniacal-N and 8.3% and 7.7% nitrate-N by MgHAU and ZnHAU, respectively within first 72 h of incubation. After six days of incubation,

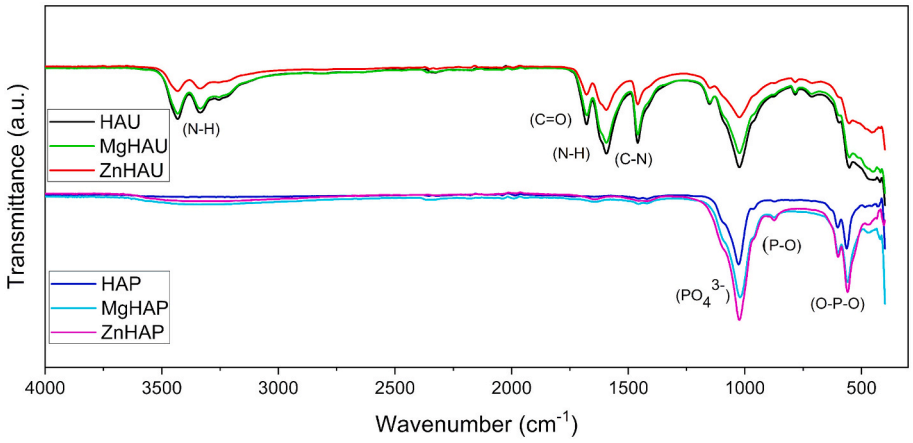


**Fig. 2.** Fourier Transform Infrared (FTIR) spectrum of synthesized nanohybrids (HAU, MgHAU and ZnHAU) and bare nanoparticles (HAP, MgHAP and ZnHAP).

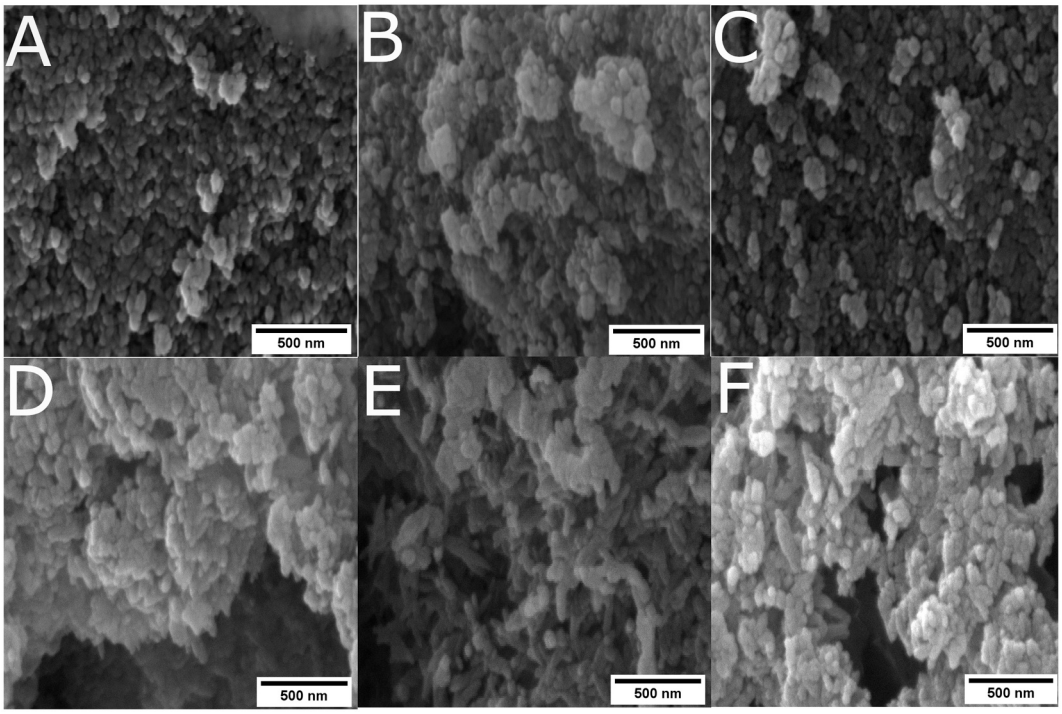


**Fig. 3.** Scanning Electron Microscopy (SEM) images of the synthesized nanomaterials A) HAP, B) MgHAP, C) ZnHAP, D) HAU, E) MgHAU, and F) ZnHAU.

ammoniacal-N release from HAU (4.6%), MgHAU (6.1%), and ZnHAU (6.5%) were significantly controlled compared to the urea (26%). In contrast, the nitrate-N release was 13.2% from urea compared to 8.4%, 10%, and 9.9% for HAU, MgHAU, and ZnHAU, respectively.

After 42 days of incubation, ammoniacal-N and nitrate-N release from urea were 26.7% and 15.2%, respectively. Surprisingly, the ammoniacal-N volatilization was largely diminished in the nanohybrids. It has been estimated that globally, up to 64% of total applied nitrogen is lost as ammonia, which directly contributes to environmental pollution (Pan et al., 2016). The total liberation of nitrogen from HAU, MgHAU, and ZnHAU was observed to be 38.45%, 44.24%, and 44.46%, respectively, compared with 97.32% from the urea fertilizer. The ammoniacal-N from urea is commonly released and volatilized rapidly from the soil, while the nitrate-N is accumulated in the soil (Pan et al., 2016; Xu et al., 2019). The ammoniacal-N liberation was reduced by at least three times compared with urea in nanohybrids. Therefore, using nanohybrids in agriculture can directly reduce ammonia greenhouse gas emissions in the environment (Sharma et al., 2022a). Our study shows that 73% of the total nitrogen from urea was rapidly released within 72 h of soil incubation compared with 16.5%, 30.2%, and 29.4% from HAU, MgHAU, and ZnHAU, respectively. Furthermore, the urea fertilizer released >90% nitrogen within seven days of incubation, whereas over the same time period, HAU, MgHAU, and ZnHAU nanohybrids released 34%, 40.3%, and 40.6% nitrogen.

Urea molecules are least endothermic in a water environment, and they form hydrogen-bonded cyclic dimers (House and House, 2017; Lee et al., 1995) that, following the density functional theory, further dissociate into monomers in the presence of abundant water molecules (Lee et al., 1995). The release of urea molecules in water is a rapid reaction as hydrogen bonding among urea molecules is lesser and weaker than that for water molecules. However, water molecules require a relatively large amount of hydrogen bond energies to break the interaction of urea with doped and undoped hydroxyapatite nanoparticles. This process delays the release of urea molecules from the surface of nanoparticles and necessitates the presence of a substantial volume of water molecules for a certain period (Sharma et al., 2022a). The urea

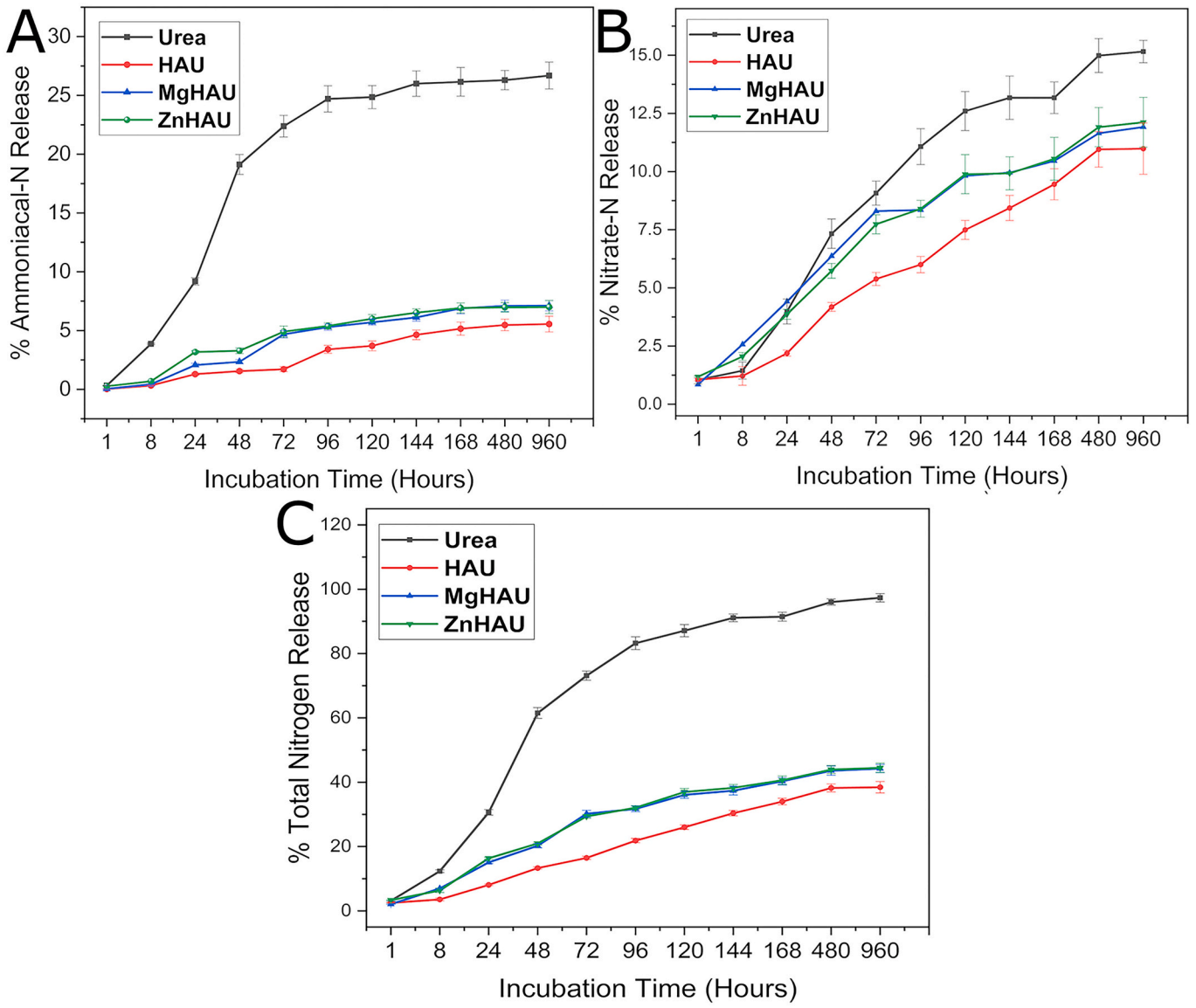


**Fig. 4.** Nitrogen release pattern in soil. A) Ammoniacal-nitrogen, B) Nitrate-nitrogen, and C) Total nitrogen release pattern of the synthesized nanohybrids (HAU. MgHAU, and ZnHAU) incubated for 42 days in the soil environment. The values are provided as mean ± standard deviation.

molecules were slowly released from our nanohybrids compared with the control due to the adsorption of water molecules onto the hydroxyapatite surfaces (Pan et al., 2007). Also, as pointed out by (Zahn and Hochrein, 2003) the formation of embedded calcium triangles that prevent water from interacting with apatite hydroxyl ions could lead to reduced exposure to water.

The water molecules diffuse anisotropically within HAP and are influenced by the strong polarizing effect of the calcium, phosphate, and hydroxyl ions (Prakash et al., 2017). Therefore, the urea dissolution in water could be hampered due to the presence of HAP nanoparticles. The zinc and magnesium doped nanohybrids disrupt the crystalline structure of hydroxyapatite and possibly damage the embedding calcium triangles that could facilitate interfacial water molecules interacting with apatite hydroxyl ions (Zahn and Hochrein, 2003). Such a modification could influence nanohybrid hydration layers and ultimately lead to an altered nitrogen release pattern. Urea burst releases nitrogen into the soil, and all the nitrogen is not likely to be utilized by the plant simultaneously. Subsequently, a substantial amount of nitrogen may be lost via volatilization or leaching (Pan et al., 2016), while slow-release would ensure the timely availability of nitrogen for uptake by plants. As demonstrated, nanohybrids dramatically reduce ammoniacal nitrogen loss and make nitrogen continuously available for plant uptake, providing increased crop yield and better grain quality (Sharma et al., 2022a).

### 3.3. Nanohybrids improve wheat growth parameters

Total nitrogen loading of 36%, 41%, and 42% was obtained for HAU, ZnHAU, and MgHAU nanohybrids, respectively. The agronomic traits and yield parameters of nanohybrid-treated wheat plants were significantly improved compared to the traditional urea-treated plants (Table S1). Plant height at 60 days was improved by 9.46% following the ZnHAU-100 nanohybrids treatment. Surprisingly, even a 50% dose of nitrogen as HAU, MgHAU, and ZnHAU maintained plant height, spike length, and effective tillers at an early growth stage.

The intensity of leaf greening is directly proportional to leaf chlorophyll content and, thus, an indicator of plant health, growth and photosynthetic capacity (Gitelson and Merzlyak, 1996). In our field experiments, the one-time application of the half doses of nitrogen as nanohybrids maintained consistently high chlorophyll levels indicating the timely availability of nitrogen for wheat growth. The leaf area of the

nano-fertilizer treated plants remained similar to those of controls except for ZnHAU-100, which showed a 13.52% increment. Increased leaf area can be closely correlated with enhanced vegetative growth and subsequent crop yield (Fischer and Kohn, 1966). Zinc and phosphorus nutrients enhance wheat crop leaf area, which can be attributed to a faster growth rate, higher chlorophyll content, and greater tiller formation (Bharti et al., 2014; Martins et al., 2015).

Similarly, the biological yield (plant weight per meter square area) was significantly increased by about 20.7% in the HAU-100 treatment. The data shows a clear and positive impact on wheat crop growth of treatment with the slow nutrient-releasing nanohybrids. Notably, the 1000 grain weight was boosted by up to 11.52% following nano-fertilizer treatments. As has been previously shown (Sharma et al., 2022a), the Zn- and Mg-doped hydroxyapatite-urea nanohybrids thus provided an optimum and timely nitrogen release that improved wheat growth and yield parameters.

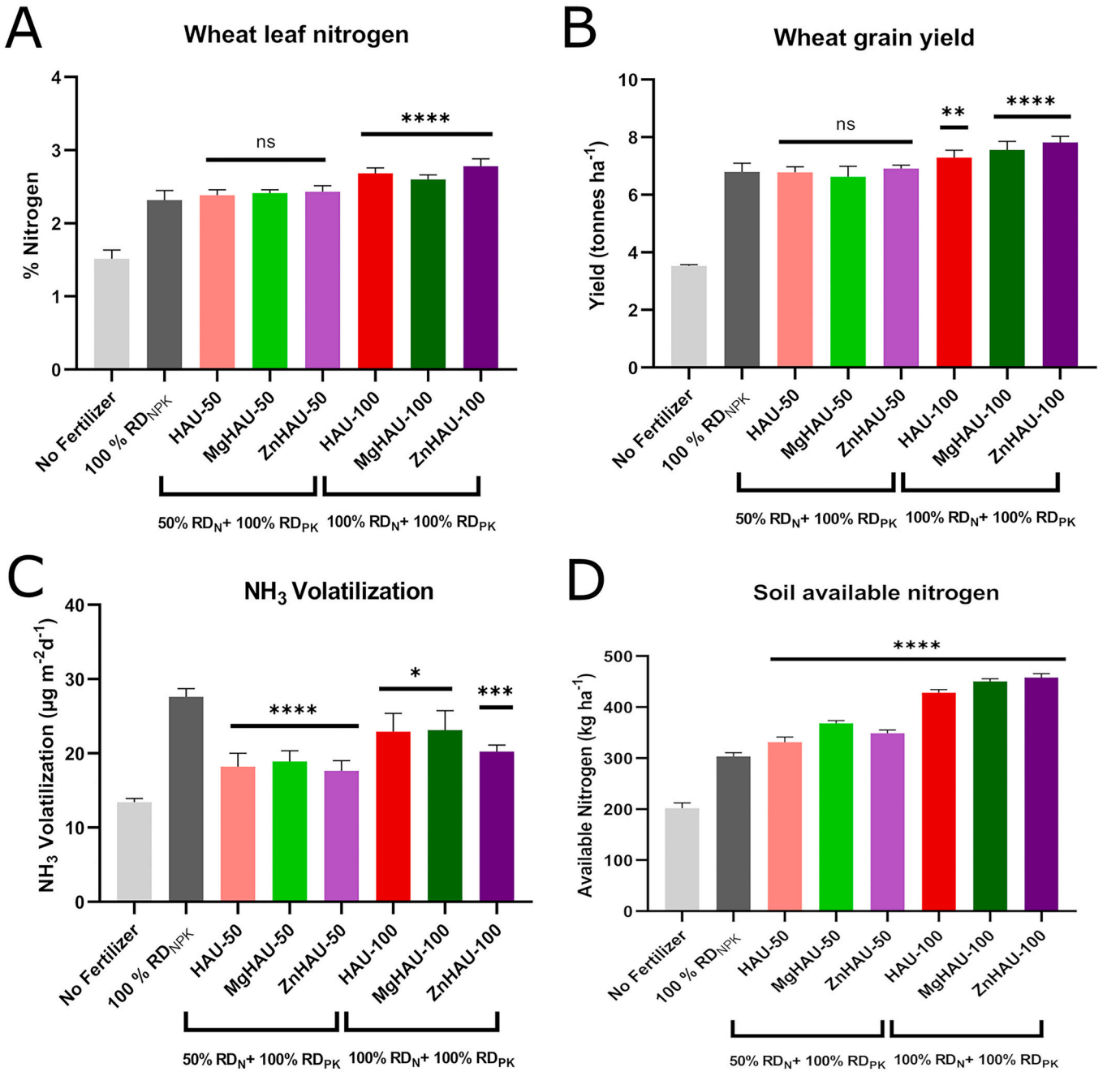


**Fig. 5.** Wheat nitrogen uptake, grain yield, ammonia volatilization and soil available nitrogen. A) Wheat leaf nitrogen, B) Wheat grain yield, C) Ammonia volatilization (µg $m^{-2}$ $d^{-1}$) from the soil, and D) Soil available nitrogen in the wheat crop cycle administered with synthesized HAU, MgHAU, and ZnHAU nanohybrids (50% and 100% nitrogen doses as nanohybrids), control (100% nitrogen as urea), and no fertilizer treatments. All the nanohybrid treatments are compared with the control or 100% $RD_{NPK}$ treatment. The values are provided as mean ± standard deviation and statistical significance was calculated by one-way ANOVA with Dunnett's multiple comparison test. The symbols '*', '**', '***', and '****' represent '$p < 0.05$', '$p < 0.01$', '$p < 0.001$', and '$p < 0.0001$', respectively and 'ns' represents 'not significant'.

### 3.4. Nanohybrids reduce nitrogen pollution and boost the nutrients uptake and crop yield in wheat

Leaf nitrogen analysis revealed an exceptional surge in wheat leaves up to 58.30% and 38.80% following HAU-100 and ZnHAU-100 treatments, respectively (Fig. 5A). Surprisingly, half-nitrogen doses as HAU enhanced nitrogen uptake by 51.35% in leaf tissues. The half-nitrogen dose of the nano-fertilizers raised nitrogen accumulation by 32.06%, whereas the full-nitrogen dose of nanohybrid increased nitrogen levels by 43.91% in the grains (Table S2). The results suggest that slowly releasing nitrogen could sufficiently supply nitrogen to the plants at both crown root initiation and tillering stages of growth, leading to enhanced nitrogen uptake and growth.

The grain yield was boosted by 22.13% in the ZnHAU-100, 7.04% in HAU-100, and 9.88% in MgHAU-100 treatments compared to controls (Fig. 5B). The nitrogen requirement at tiller formation, during stem elongation, and at grain filling are crucial for enhanced growth and yield of wheat (Weisz et al., 2001; Alley et al., 2009). Interestingly, half-nitrogen doses of nano fertilizers maintained crop yield at the same or higher levels as the full nitrogen dose of conventional urea fertilizer treatments.

The mean ammonia volatilization from the soil was significantly reduced by up to 36% in the nanohybrid treatments compared with control treatments (Fig. 5C). Urea hydrolysis is assisted by the urease enzyme that generates ammonium carbonate and dissociates into ammonium ($NH_4^+$) and bicarbonate ($HCO_3^-$) (Sigurdarson et al., 2018). The bicarbonate ion absorbs surrounding $H^+$ ions that increase the pH above 7, and the ammonium ion ($NH_4^+$) is converted into ammonia gas ($NH_3$) which is released into the atmosphere. Our results suggest that nanohybrids could protect the surface-bound urea from urease activity and minimize nitrogen losses. The nanohybrids therefore reduce the level of nitrogen fertilizer required and limit nitrogen emissions into the atmosphere.

Pure urea-treated soil consumed all the applied nitrogen fertilizer while full dose nanohybrids treatments retained a large amount of nitrogen in the soil (Fig. 5D). Overall, the available nitrogen levels were relatively high in the nanohybrid-treated soil with the sustainable release of nitrogen from nanohybrids, and with a substantial amount of nitrogen maintained in the soil that could be used for consecutive crop cycles. The nitrogen release from the nanohybrids was prolonged in later crop growth stages because as urea molecules were removed from the surface of nanoparticles, the remaining urea molecules were firmly held through abundant surface interactions nanoparticles (Sharma et al., 2022a). These findings are supported by the nitrogen release kinetics study and serve as strong evidence for applying slow-release nitrogen fertilizer for successful and sustainable agriculture.

Phosphorus uptake was increased in the wheat grain (by up to 41.43%), and roots (by up to 54.62%) tissues in the nanohybrid fertilizer-treated crop (Table S2). The hydroxyapatite nanoparticles either dissolve in the root epidermis and apoplast to release phosphorus and other nutrients, or nanoparticles could degrade in the soil and phosphorus released in the soil was taken up by plants (Montalvo et al., 2015; Liu and Lal, 2014; Szameitat et al., 2021). The potassium levels were improved in grains and stem following full-dose nanohybrid treatments (Table S2). Similarly, the calcium levels were surprisingly raised in the grains of nanohybrid-treated plants, especially for the HAU treatments (up to 180.86%) (Table S2). Magnesium content was substantially increased in the grain (up to 175.54%) and root (up to 142.10%) tissues following full-dose nanohybrid treatments (Table S2). Zinc levels were increased by up to 30% in the grains following full-dose nanohybrid treatment (Table S3).

Zinc, magnesium, calcium, phosphorus, and nitrogen were delivered as nanohybrids, and we observed improved uptake of these nutrient elements. Interestingly, even though they were not present in the nanohybrids, enhanced uptake of iron and manganese elements was found in plant tissues (Table S3). Iron and manganese uptake was boosted up to 266.99% and 34.56%, respectively, in the grains of nanohybrid-treated plants (Table S3). The manganese level in the root tissues was increased by up to 14.76% in half-dose nanohybrids. Due to their excellent sorption capacities, an additional uptake of iron and manganese by the plants may have resulted from soil nutrient adsorption onto the hydroxyapatite nanoparticles (El kady et al., 2016). These results reflect further and additional benefits to crops of nanohybrid application to the soil.

Moreover, the protein content was remarkably improved in grain tissue following nanohybrid treatments (Table S4). We observed at least a two-fold increment in all the nanohybrid treated grain proteins. The HAU-50 and HAU-100, and MgHAU-100 showed increased levels of phospholipids up to 5.05% compared with the control. The proline content was enhanced significantly by 39.60% in MgHAU-100. The improvement in the grain protein, phospholipid, and proline content (Table S4) in the nanohybrid-treated plants confirmed the beneficial impact of slow-release nitrogen on grain quality (Martin et al., 1992). Our study has thus demonstrated that applying the synthesized engineered nanohybrids as a fertilizer result in enhanced crop growth and promotes biofortification. The nano fertilizer could save up to half the amount of nitrogen fertilizer generally applied to a crop for an equivalent or better crop yield and, remarkably, still be available in the soil for the next crop cycle.

### 3.5. Nanohybrids exhibit no adverse impact on soil microbial activity

The urease and dehydrogenase activity of the soil treated with nanohybrids was tested to assess the impact on soil microbial activity (Fig. 6). Soil dehydrogenase enzyme activity is an indicator of soil microbial activities and is influenced by several environmental factors such as temperature, pH, substrate concentration, and inorganic nitrogen (Trevors, 1984). We observed that soil microbial activities were significantly enhanced in Zn- and Mg-HAU nanohybrid treatments compared to control and HAU treatments (Fig. 6A and B). The dehydrogenase activity was exceptionally enhanced to 409.97% and 534.55% above controls at 0–15 cm and 15–30 cm soil depth, respectively, for the ZnHAU-50 treatments.

Urease activity in the soil is responsible for urea transformation and making it available for plant uptake. Soil urease activity is attributed to a complex of factors, including vegetation type, organic carbon, total nitrogen, and microbial proliferation and activity (Rao and Ghai, 1985). The urease activity at the 0–15 cm soil depth in our experiments was enhanced in the HAU and ZnHAU treatments by up to 33.88% and 20.07%, respectively, compared to the control (Fig. 6C). Similarly, the 100% nanohybrids (up to 81.82%) and ZnHAU-50 treatments (41.55%) boosted the urease activity at the 15–30 cm soil depth (Fig. 6D). Urease activity is usually suppressed in calcareous soils (Zantua et al., 1977), but in our study, we observed that despite the presence of a calcium-based backbone of the hydroxyapatite nanohybrids, soil urease activity was enhanced. These results suggest a beneficial impact of the doped nanohybrids, especially ZnHAU nanohybrids, on soil microbial population, and that the nanohybrids can be applied to the soil for large-scale agricultural production without damaging soil microbial activity (Sharma et al., 2022a).

### 3.6. Residual nitrogen derived from nanohybrid improves rice growth and nutrient uptake in a second and subsequent crop cycle

The assessment of residual nitrogen was an essential factor in this study because, after the wheat growth cycle, the soil available nitrogen levels in nano-fertilizer treatments were unexpectedly higher than in urea treatments. Therefore, we conducted a follow-up rice crop trial to examine the efficacy of the residual nitrogen in the nanohybrid-treated soil.

The plant height of the rice paddy was significantly improved between 16.66% to 26.34% in the nano-fertilizer treatments (Table S5).

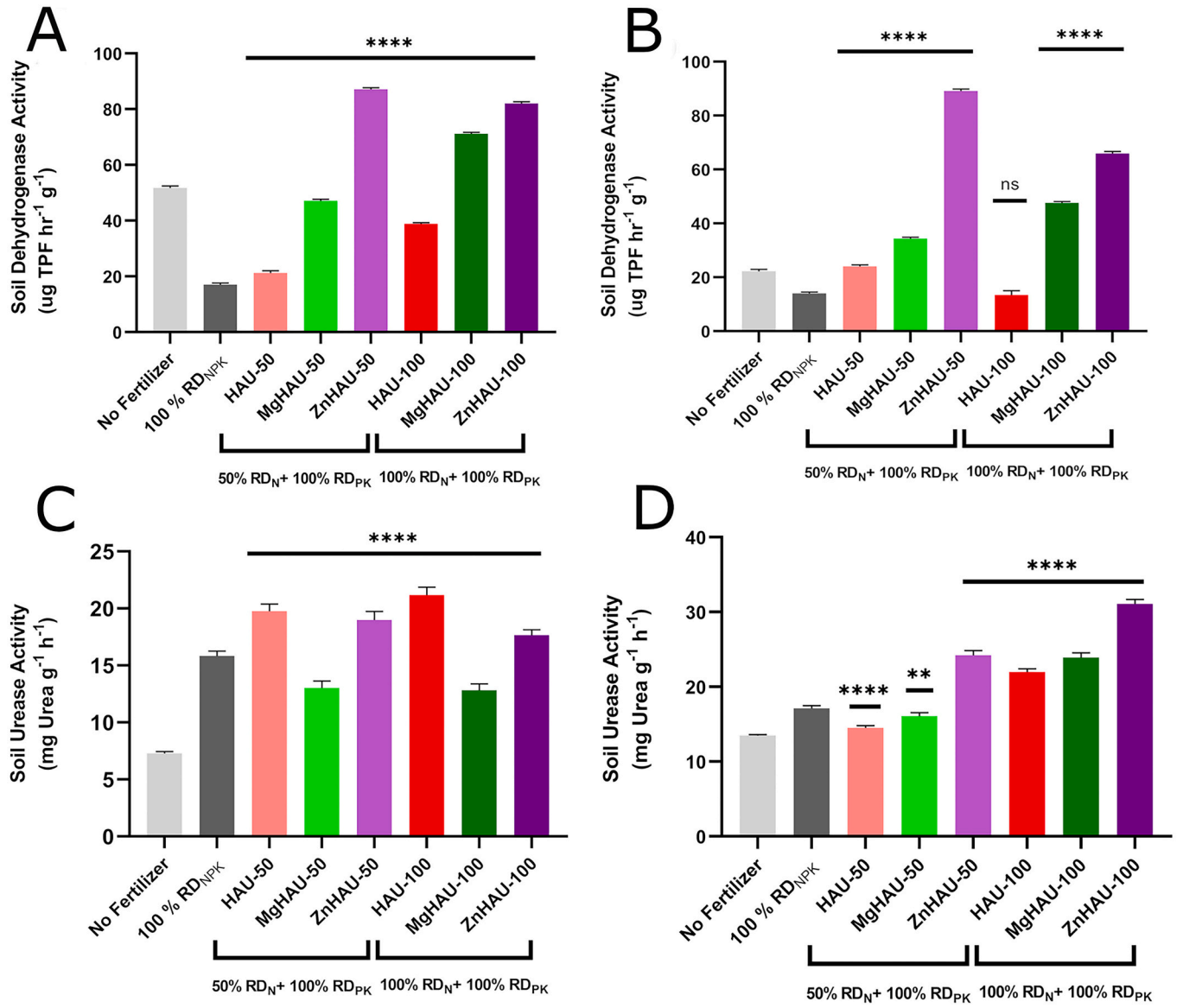


**Fig. 6.** Dehydrogenase and urease activity in nanohybrids treated soil. A) Soil Dehydrogenase activity (0–15 cm soil depth), B) Soil Dehydrogenase activity (15–30 cm soil depth), C) Soil Urease activity (0–15 cm soil depth), and D) Soil Urease activity (15–30 cm soil depth) assessment in the soil treated with synthesized HAU, MgHAU, and ZnHAU nanohybrids (50% and 100% nitrogen doses as nanohybrids), control (100% nitrogen as urea), and no fertilizer treatments after wheat crop cycle. All the nanohybrid treatments are compared with the control or 100% $RD_{NPK}$ treatment. The values are provided as mean ± standard deviation and statistical significance was calculated by one-way ANOVA with Dunnett's multiple comparison test. The symbols '*', '**', '***', and '****' represent '$p < 0.05$', '$p < 0.01$', '$p < 0.001$', and '$p < 0.0001$', respectively and 'ns' represents 'not significant'.

The tiller numbers and panicle lengths were enhanced up to 13.37% and 21.83%, respectively, in the nanohybrid treatments (Table S5). Panicle length was improved in MgHAU (up to 20.52%), ZnHAU (up to 21.83%) and HAU (up to 9.1%) treatments compared with the control (Table S5). Similarly, the number of grains per panicle increased significantly by 40% in the nanohybrid treatments (Table S5). Furthermore, 1000-grain weight was improved in all the nano fertilizer treatments with maximum yield in ZnHAU-100 nanohybrids (an increase of up to 16.10%) (Table S5).

Leaf nitrogen in the 40-day-old rice plants was significantly enhanced (up to 18%) in the ZnHAU-50 and ZnHAU-100 treatments while maintained in the HAU-50 and MgHAU-50 treatments (Fig. 7A). An improved leaf nitrogen uptake at an early growth stage of the rice plant indicates timely availability and slow release of nitrogen from nanohybrids during the consecutive and second crop cycle. The crop biological weight, straw weight, and crop yield were significantly enhanced in all the nanohybrid treatments compared to the control treatment (Table S5 and Fig. 7B). Surprisingly, there was up to a 119.23%, 118.31%, and 72.50% increase in biological weight, straw-weight, and crop yield, respectively, in the ZnHAU treatments above that of the control-treated rice crop (Table S5 and Fig. 7B).

After harvesting the crop, the rice grain, stem, and root tissues were analyzed for their macro-and micro-nutrient uptake (Table S6 and S7). The nitrogen level in rice grains was increased by 154.71% in the nanohybrid treatments compared to the urea-treated rice crop grains (Table S5). Similarly, rice roots and stem tissues showed an elevated nitrogen level of up to 79.45% and up to 50.42%, respectively, compared with the control (Fig. 7B).

Rice crops prefer ammoniacal nitrogen as a nitrogen source (Duan et al., 2007) and the nanohybrids mitigated ammoniacal nitrogen volatilization, which is then available for plant uptake. The mean ammonia volatilization was estimated for the rice crop season, revealing

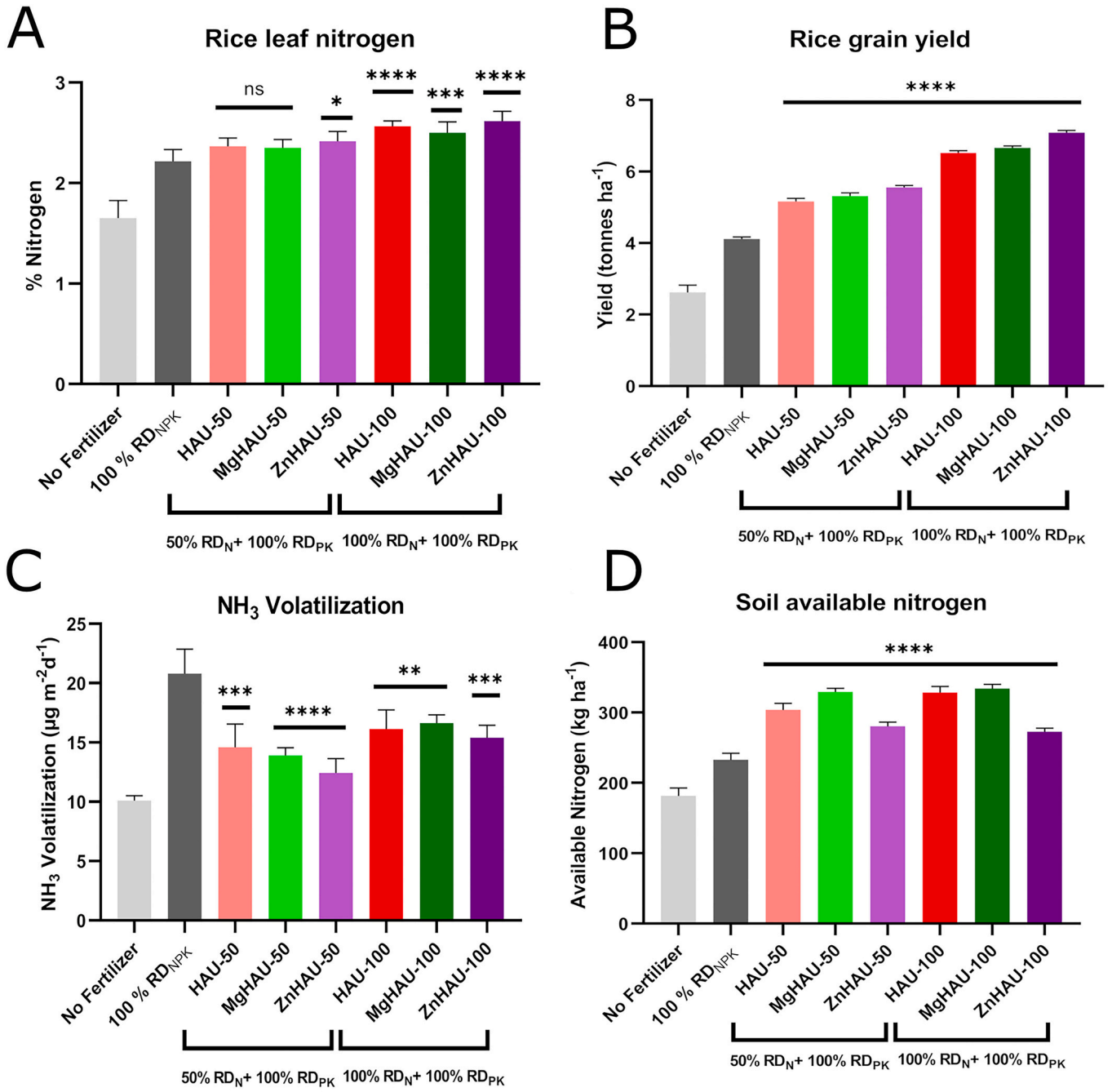


**Fig. 7.** Rice nitrogen uptake, grain yield, ammonia volatilization and soil available nitrogen. A) Rice leaf nitrogen, B) Rice grain yield, C) Mean ammonia volatilization (µg $m^{-2}$ $d^{-1}$) from the soil, and D) Soil available nitrogen in the rice crop cycle administered with synthesized HAU, MgHAU, and ZnHAU nanohybrids (50% and 100% nitrogen doses as nanohybrids), control (100% nitrogen as urea), and no fertilizer treatments. All the nanohybrid treatments are compared with the control or 100% $RD_{NPK}$ treatment. The values are provided as mean ± standard deviation and statistical significance was calculated by one-way ANOVA with Dunnett's multiple comparison test. The symbols '*', '**', '***', and '****' represent '$p < 0.05$', '$p < 0.01$', '$p < 0.001$', and '$p < 0.0001$', respectively and 'ns' represents 'not significant'.

a significant reduction (up to 67.29%) in the ammonia losses from all the nanohybrid treatments (Fig. 7C). The abundant availability (up to 329.56%) of the slow-releasing ammoniacal nitrogen could be a driving factor for better nitrogen uptake and the boost found in crop growth (Fig. 7D).

Rice grain phosphorus content was significantly improved by 8.3% to 18.39% in the nanohybrid treatments compared with controls (Table S6). The stem phosphorus uptake was enhanced in ZnHAU-100 by 17.26% and up to 31% in the root tissues. The potassium levels did not change in the nanohybrid-treated rice except for ZnHAU-100 treatments of stem and root tissues (Table S6). The calcium content increased to 40.2% in the full-dose nanohybrid treated root tissues and did not change in the grain (Table S6) and stem tissues. Magnesium accumulation was improved in the doped nanohybrids treated grain (up to 34.26%) (Table S6) and in the 100% nitrogen doses of nanohybrid treated root tissues (up to 80.43%).

Similarly, zinc uptake was enhanced up to 52.51% in the 100% nanohybrids and ZnHAU-50 treated rice grains (Table S7). Zinc content was exclusively increased in the ZnHAU-50 (9.3%) and ZnHAU-100 (16.56%) treatments. Likewise, the zinc content was enhanced in

MgHAU-100, and ZnHAU-100 treated rice root tissues by 9.27% and 14.18%, respectively.

Surprisingly, iron uptake was enhanced in the nanohybrid-treated rice grains of ZnHAU-50 (13.87%), MgHAU-100 (17.7%), and ZnHAU-100 (26.31%) treatments (Table S7). Iron uptake was also increased in the tissues of the stem (up to 58.18%) and root (up to 43.75%). Similarly, the manganese content was enhanced up to 14.15% in the grains of doped hydroxyapatite-urea treated stem tissues (Table S7).

Compared with the burst release of nitrogen from urea, the slow nitrogen release from nanoparticles reduced nitrogen inputs. The use of nanohybrids could substantially reduce nitrogen loss from the soil and, instead, preferentially supply the rice crop with ammoniacal nitrogen slowly over a longer time period (Shen, 1969). The cost of the nanohybrids produced in the laboratory was approximately 30–40% higher than the urea fertilizers. But this cost can further be reduced by half with the demonstrated efficacy of the nitrogenous nanohybrids for nitrogen and additional nutrient delivery to crops.

The present study exemplifies that a comprehensive understanding is required of the synthesis, characterization, and application of slow-release nitrogen nanohybrids, preferably over two or more consecutive crop cycles. Thus, these nanohybrids can serve as a multi-nutrient source for plant growth while reducing the overall amount of nitrogen application to agricultural fields for their use in sustainable agriculture while minimizing their impact on the environment.

## 4. Conclusion

The excess application of nitrogen in the form of chemical fertilizer to agricultural fields promotes environmental pollution and contributes to climate change. The application of chemical fertilizers should be regulated to mitigate environmental consequences. We have synthesized Mg and Zn doped and undoped hydroxyapatite nanohybrids functionalized with nitrogen fertilizer that control the release of nitrogen for a timely, efficient and sufficient supply to crops. The nanohybrids significantly reduced nitrogen loss in the environment. We observed that even a half concentration of such eco-friendly nutrient complexes enhanced the bioavailability of nitrogen, enhancing crop growth and nutrient uptake for at least two crop cycles. Our synthesized nanohybrids can be a revolutionary tool that will contribute to the alleviation of the pollution and waste generation arising from agriculture. These doped nanohybrids were multi-nutrient complexes that biofortified the crops with minimum fertilizer, making agriculture less costly and safer for the environment. We also demonstrated the novel use of the doping method to integrate micro-nutrients into nanoparticles for the dual purpose of manipulating nanostructures and micro-nutrient delivery. The present study thus establishes comprehensive experimental evidence for the two-crop cycle application of nano-fertilizers. It unlocks new paradigms for designing and applying climate-friendly smart fertilizers for sustainable agriculture.

## Funding information

BS was supported by a Deakin University Postgraduate Scholarship.

## CRediT authorship contribution statement

**Bhaskar Sharma:** Conceptualization, Methodology, Investigation, Data curation, Formal analysis, Validation, Visualization, Writing – original draft, Writing – review & editing. **Manoj Shrivastava:** Supervision, Writing – review & editing. **Luis O.B. Afonso:** Supervision, Writing – review & editing. **Udit Soni:** Supervision, Conceptualization, Writing – review & editing. **David M. Cahill:** Supervision, Conceptualization, Writing – review & editing.

## Declaration of Competing Interest

The authors declare that they have no known competing financial interests.

## Data availability

Data used in the study was provided in this article and its supplementary data.

## Acknowledgments

Authors thank Deakin University, Australia, and TERI School of Advanced Studies, India for providing necessary infrastructure and research facilities. Authors are thankful to Indian Agricultural Research Institute, India for providing necessary resources and assistance in the field experiments. Authors are grateful to Dr. Chaithanya Madhurantakam, Associate Professor, TERI SAS for providing basic research facilities. Authors thank JNU AIRF, Delhi and AIIMS SAIF, Delhi for XRD, FTIR, SEM, TEM, and EDX facilities. Graphical abstract was created with BioRender.com

## Appendix A. Supplementary data

Cryo-TEM (Fig. S1), EDX (Fig. S2), Hydrodynamic diameter and zeta potential (Table S1), Wheat growth and yield parameters (Table S2), Macro- and Micro-nutrients levels in wheat tissues (Table S3, Table S4), Protein, proline, and phospholipids (Grain quality) estimation (Table S5), Rice growth and yield parameters (Table S6), Macro- and Micro-nutrients levels in rice tissues (Table S7, Table S8).

## References

Alexandratos, N., Bruinsma, J., 2012. World Agriculture towards 2030/2050: The 2012 Revision.
Alley, M.M., Scharf, P.C., Brann, D.E., Baethgen, W.E., Hammons, J., 2009. Nitrogen Management for Winter Wheat: Principles and Recommendations.
Avellan, A., Yun, J., Morais, B.P., Clement, E.T., Rodrigues, S.M., Lowry, G.V., 2021. Critical review: role of inorganic nanoparticle properties on their foliar uptake and in planta translocation. Environ. Sci. Technol. 55, 13417–13431.
Aziz, H.M.A., Hasaneen, M.N., Omer, A.M., 2016. Nano chitosan-NPK fertilizer enhances the growth and productivity of wheat plants grown in sandy soil. Span. J. Agric. Res. 14, 17.
Bahrami, N., Yonekura, L., Linforth, R., Carvalho, D.A., Silva, M., Hill, S., Penson, S., Chope, G., Fisk, I.D., 2014. Comparison of ambient solvent extraction methods for the analysis of fatty acids in non-starch lipids of flour and starch. J. Sci. Food Agric. 94, 415–423.
Bansiwal, A.K., Rayalu, S.S., Labhasetwar, N.K., Juwarkar, A.A., Devotta, S., 2006. Surfactant-modified zeolite as a slow release fertilizer for phosphorus. J. Agric. Food Chem. 54, 4773–4779.
Bates, L.S., Waldren, R.P., Teare, I., 1973. Rapid determination of free proline for water-stress studies. Plant Soil 39, 205–207.
Bharti, K., Pandey, N., Shankhdhar, D., Srivastava, P.C., Shankhdhar, S.C., 2014. Effect of exogenous zinc supply on photosynthetic rate, chlorophyll content and some growth parameters in different wheat genotypes. Cereal Res. Commun. 42, 589–600.
Bouyoucos, G.J., 1962. Hydrometer method improved for making particle size analyses of soils 1. Agron. J. 54, 464–465.
Brealey, L., 1951. The determination of potassium in fertilisers by flame photometry. Analyst 76, 340–343.
Bremner, J., 1960. Determination of nitrogen in soil by the Kjeldahl method. J. Agric. Sci. 55, 11–33.
Cameron, K., Di, H.J., Moir, J., 2013. Nitrogen losses from the soil/plant system: a review. Ann. Appl. Biol. 162, 145–173.
Compton, S.J., Jones, C.G., 1985. Mechanism of dye response and interference in the Bradford protein assay. Anal. Biochem. 151, 369–374.
Dasgupta, S., Banerjee, S.S., Bandyopadhyay, A., Bose, S., 2010. Zn- and Mg-doped hydroxyapatite nanoparticles for controlled release of protein. Langmuir 26, 4958–4964.
Dimkpa, C.O., Fugice, J., Singh, U., Lewis, T.D., 2020. Development of fertilizers for enhanced nitrogen use efficiency–trends and perspectives. Sci. Total Environ. 731, 139113.
Dinarvand, P., Seyedjafari, E., Shafiee, A., Babaei Jandaghi, A., Doostmohammadi, A., Fathi, M.H., Farhadian, S., Soleimani, M., 2011. New approach to bone tissue engineering: simultaneous application of hydroxyapatite and bioactive glass coated on a poly (L-lactic acid) scaffold. ACS Appl. Mater. Interfaces 3, 4518–4524.

Duan, Y.H., Zhang, Y.L., Ye, L.T., Fan, X.R., Xu, G.H., Shen, Q.R., 2007. Responses of rice cultivars with different nitrogen use efficiency to partial nitrate nutrition. Ann. Bot. 99, 1153–1160.
Dubey, A., Mailapalli, D.R., 2019. Zeolite coated urea fertilizer using different binders: fabrication, material properties and nitrogen release studies. Environmental Technology & Innovation 16, 100452.
EL Kady, M., Shokry, H., Hamad, H., 2016. Effect of superparamagnetic nanoparticles on the physicochemical properties of nano hydroxyapatite for groundwater treatment: adsorption mechanism of Fe(ii) and Mn(ii). RSC Adv. 6, 82244–82259.
Fischer, R.A., Kohn, G.D., 1966. The relationship of grain yield to vegetative growth and post-flowering leaf area in the wheat crop under conditions of limited soil moisture. Aust. J. Agric. Res. 17, 281–295.
Fishman, M.J., Friedman, L.C., 1989. Methods for Determination of Inorganic Substances in Water and Fluvial Sediments. US Department of the Interior, Geological Survey.
Gastal, F., Lemaire, G., 2002. N uptake and distribution in crops: an agronomical and ecophysiological perspective. J. Exp. Bot. 53, 789–799.
Gilbertson, L.M., Pourzahedi, L., Laughton, S., Gao, X., Zimmerman, J.B., Theis, T.L., Westerhoff, P., Lowry, G.V., 2020. Guiding the design space for nanotechnology to advance sustainable crop production. Nat. Nanotechnol. 15, 801–810.
Giller, K.E., Chalk, P., Dobermann, A., Hammond, L., Heffer, P., Ladha, J.K., Nyamudeza, P., Maene, L., Ssali, H., Freney, J., 2004. Emerging technologies to increase the efficiency of use of fertilizer nitrogen. Agriculture and the nitrogen cycle: assessing the impacts of fertilizer use on food production and the environment 65, 35–51.
Gitelson, A.A., Merzlyak, M.N., 1996. Signature analysis of leaf reflectance spectra: algorithm development for remote sensing of chlorophyll. J. Plant Physiol. 148, 494–500.
Good, A.G., Beatty, P.H., 2011. Fertilizing nature: a tragedy of excess in the commons. PLoS Biol. 9, e1001124.
Hanson, W., 1950. The photometric determination of phosphorus in fertilizers using the phosphovanado-molybdate complex. J. Sci. Food Agric. 1, 172–173.
Hanway, J., Heidel, H., 1952. Soil analysis methods as used in Iowa state college soil testing laboratory. Iowa agriculture 57, 1–31.
Hofman, G., Van Cleemput, O., 2004. Soil and Plant Nitrogen.
Hofmann, T., Lowry, G.V., Ghoshal, S., Tufenkji, N., Brambilla, D., Dutcher, J.R., Gilbertson, L.M., Giraldo, J.P., Kinsella, J.M., Landry, M.P., 2020. Technology readiness and overcoming barriers to sustainably implement nanotechnology-enabled plant agriculture. Nature Food 1, 416–425.
House, K.A., House, J.E., 2017. Thermodynamics of dissolution of urea in water, alcohols, and their mixtures. J. Mol. Liq. 242, 428–432.
Huang, W.-Y., Uri, N.D., 1993. The effect of farming practices on reducing excess nitrogen fertilizer use. Environ. Int. 19, 179–191.
Hussain, S., Skopp, J., Mielke, L., 1988. Detachment of soil as affected by fertility management and crop rotations. Soil Sci. Soc. Am. J. 52, 1463–1468.
Ikemoto, Y., Teraguchi, M., Kobayashi, Y., 2002. Plasma levels of nitrate in congenital heart disease: comparison with healthy children. Pediatr. Cardiol. 23, 132–136.
Jampílek, J., Kráľová, K., 2017. Nanomaterials for Delivery of Nutrients and Growth-Promoting Compounds to Plants. Nanotechnology. Springer.
Kumar, R., Prakash, K.H., Cheang, P., Khor, K.A., 2004. Temperature driven morphological changes of chemically precipitated hydroxyapatite nanoparticles. Langmuir 20, 5196–5200.
Lee, C., Stahlberg, E.A., Fitzgerald, G., 1995. Chemical structure of urea in water. J. Phys. Chem. 99, 17737–17741.
Lindsay, W.L., Norvell, W.A., 1978. Development of a DTPA soil test for zinc, iron, manganese, and copper. Soil Sci. Soc. Am. J. 42, 421–428.
Liu, R., Lal, R., 2014. Synthetic apatite nanoparticles as a phosphorus fertilizer for soybean (*Glycine max*). Sci. Rep. 4, 5686.
Lu, J., Bai, Z., Velthof, G.L., Wu, Z., Chadwick, D., Ma, L., 2019. Accumulation and leaching of nitrate in soils in wheat-maize production in China. Agric. Water Manag. 212, 407–415.
Martin, R.J., Sutton, K.H., Moyle, T.N., Hay, R.L., Gillespie, R.N., 1992. Effect of nitrogen fertiliser on the yield and quality of six cultivars of autumn-sown wheat. N. Z. J. Crop. Hortic. Sci. 20, 273–282.
Martins, L.E.C., Monteiro, F.A., Pedreira, B.C., 2015. Photosynthesis and leaf area of *Brachiaria brizantha* in response to phosphorus and zinc nutrition. J. Plant Nutr. 38, 754–767.
Meret, S., Henkin, R., 1971. Simultaneous direct estimation by atomic absorption spectrophotometry of copper and zinc in serum, urine, and cerebrospinal fluid. Clin. Chem. 17, 369–373.
Montalvo, D., Mclaughlin, M.J., Degryse, F., 2015. Efficacy of hydroxyapatite nanoparticles as phosphorus fertilizer in Andisols and Oxisols. Soil Sci. Soc. Am. J. 79, 551–558.
Nelson, D.W., Sommers, L.E., 2020. Total nitrogen analysis of soil and plant tissues. Journal of Association of Official Analytical Chemists 63, 770–778.
Olsen, S.R., 1954. Estimation of Available Phosphorus in Soils by Extraction with Sodium Bicarbonate. US Department of Agriculture.
Padhye, V., 1957. A rapid method for the determination of calcium and magnesium in plant material by titration with disodium ethylenediaminetetra-acetate. Analyst 82, 634–638.
Pan, B., Lam, S.K., Mosier, A., Luo, Y., Chen, D., 2016. Ammonia volatilization from synthetic fertilizers and its mitigation strategies: A global synthesis. Agric. Ecosyst. Environ. 232, 283–289.
Pan, H., Tao, J., Wu, T., Tang, R., 2007. Molecular simulation of water behaviors on crystal faces of hydroxyapatite. Frontiers of Chemistry in China 2, 156–163.
Poinern, G., Brundavanam, R., Le, X.T., Djordjevic, S., Prokic, M., Fawcett, D., 2011. Thermal and ultrasonic influence in the formation of nanometer scale hydroxyapatite bio-ceramic. Int. J. Nanomedicine 6, 2083.
Prakash, M., Lemaire, T., Caruel, M., Lewerenz, M., De Leeuw, N.H., Di Tommaso, D., Naili, S., 2017. Anisotropic diffusion of water molecules in hydroxyapatite nanopores. Phys. Chem. Miner. 44, 509–519.
Predoi, D., Iconaru, S.L., Predoi, M.V., Motelica-Heino, M., Guegan, R., Buton, N., 2019. Evaluation of antibacterial activity of zinc-doped hydroxyapatite colloids and dispersion stability using ultrasounds. Nanomaterials 9 (4), 515. https://doi.org/10.3390/nano9040515.
Raimbault, B., Vyn, T., 1991. Crop rotation and tillage effects on corn growth and soil structural stability. Agron. J. 83, 979–985.
Rao, D., Ghai, S., 1985. Urease and dehydrogenase activity of alkali and reclaimed soils. Soil Research 23, 661–665.
Reddy, K., Patrick, W., Broadbent, F., 1984. Nitrogen transformations and loss in flooded soils and sediments. Crit. Rev. Environ. Sci. Technol. 13, 273–309.
Sagle, L.B., Zhang, Y., Litosh, V.A., Chen, X., Cho, Y., Cremer, P.S., 2009. Investigating the hydrogen-bonding model of urea denaturation. J. Am. Chem. Soc. 131, 9304–9310.
Sapkota, T.B., Singh, L.K., Yadav, A.K., Khatri-Chhetri, A., Jat, H.S., Sharma, P.C., Jat, M. L., Stirling, C.M., 2020. Identifying optimum rates of fertilizer nitrogen application to maximize economic return and minimize nitrous oxide emission from rice–wheat systems in the Indo-Gangetic Plains of India. Arch. Agron. Soil Sci. 66, 2039–2054.
Setty, K.E., Kayser, G.L., Bowling, M., Enault, J., Loret, J.-F., Serra, C.P., Alonso, J.M., Mateu, A.P., Bartram, J., 2017. Water quality, compliance, and health outcomes among utilities implementing Water Safety Plans in France and Spain. Int. J. Hyg. Environ. Health 220, 513–530.
Severenghaus, J., Ferrebee, J., 1950. Calcium determination by flame photometry; methods for serum, urine, and other fluids. J. Biol. Chem. 187, 621–630.
Sharma, B., Shrivastava, M., Afonso, L.O.B., Soni, U., Cahill, D.M., 2022a. Zinc- and Magnesium-Doped Hydroxyapatite Nanoparticles Modified with Urea as Smart Nitrogen Fertilizers. ACS Applied Nano Materials.
Sharma, B., Soni, U., Afonso, L.O., Cahill, D.M., 2022b. Nanomaterial Doping: Chemistry and Strategies for Agricultural Applications. ACS Agricultural Science & Technology.
Shen, T., 1969. The induction of nitrate reductase and the preferential assimilation of ammonium in germinating rice seedlings. Plant Physiol. 44, 1650–1655.
Sigurdarson, J.J., Svane, S., Karring, H., 2018. The molecular processes of urea hydrolysis in relation to ammonia emissions from agriculture. Rev. Environ. Sci. Biotechnol. 17, 241–258.
Songkhum, P., Wuttikhun, T., Chanlek, N., Khemthong, P., Laohhasurayotin, K., 2018. Controlled release studies of boron and zinc from layered double hydroxides as the micronutrient hosts for agricultural application. Appl. Clay Sci. 152, 311–322.
Srivastava, A.K., Singh, S., 2009. Citrus decline: soil fertility and plant nutrition. J. Plant Nutr. 32, 197–245.
Stumpe, J.M., Vlek, P., Lindsay, W., 1984. Ammonia volatilization from urea and urea phosphates in calcareous soils. Soil Sci. Soc. Am. J. 48, 921–927.
Subbaiah, B., 1956. A rapid procedure for estimation of available nitrogen in soil. Curr. Sci. 25, 259–260.
Subhaiaih, B., Asija, G., 1956. A rapid procedure for estimation of available nitrogen in soils. Curr. Sci. 25, 259–260.
Szameitat, A.E., Sharma, A., Minutello, F., Pinna, A., Er-rafik, M., Hansen, T.H., Persson, D.P., Andersen, B., Husted, S., 2021. Unravelling the interactions between nano-hydroxyapatite and the roots of phosphorus deficient barley plants. Environmental Science: Nano 8, 444–459.
Tao, J., Pan, H., Zeng, Y., Xu, X., Tang, R., 2007. Roles of amorphous calcium phosphate and biological additives in the assembly of hydroxyapatite nanoparticles. J. Phys. Chem. B 111, 13410–13418.
Tilman, D., Cassman, K.G., Matson, P.A., Naylor, R., Polasky, S., 2002. Agricultural sustainability and intensive production practices. Nature 418, 671–677.
Tilman, D., Balzer, C., Hill, J., Befort, B.L., 2011. Global food demand and the sustainable intensification of agriculture. Proc. Natl. Acad. Sci. 108, 20260–20264.
Trenkel, M.E., 1997. Controlled-Release and Stabilized Fertilizers in Agriculture. International fertilizer industry association Paris.
Trevors, J.T., 1984. Effect of substrate concentration, inorganic nitrogen, O2 concentration, temperature and pH on dehydrogenase activity in soil. Plant Soil 77, 285–293.
Van Dijk, M., Morley, T., Rau, M.L., Saghai, Y., 2021. A meta-analysis of projected global food demand and population at risk of hunger for the period 2010–2050. Nature Food 2, 494–501.
Walkley, A., Black, I.A., 1934. An examination of the Degtjareff method for determining soil organic matter, and a proposed modification of the chromic acid titration method. Soil Sci. 37, 29–38.
Wang, Z., Zong, Z., Li, S., Chen, B., 2002. Nitrate accumulation in vegetables and its residual in vegetable fields. Huan jing ke xue= Huanjing kexue 23, 79–83.
Weisz, R., Crozier, C.R., Heiniger, R.W., 2001. Optimizing nitrogen application timing in no-till soft red winter wheat. Agron. J. 93, 435–442.
Xu, R., Tian, H., Pan, S., Prior, S.A., Feng, Y., Batchelor, W.D., Chen, J., Yang, J., 2019. Global ammonia emissions from synthetic nitrogen fertilizer applications in agricultural systems: empirical and process-based estimates and uncertainty. Glob. Chang. Biol. 25, 314–326.
Yadav, S.N., 1997. Formulation and estimation of nitrate-nitrogen leaching from corn cultivation. J. Environ. Qual. 26, 808–814.
Yoon, H.Y., Lee, J.G., Esposti, L.D., Iafisco, M., Kim, P.J., Shin, S.G., Jeon, J.-R., Adamiano, A., 2020. Synergistic release of crop nutrients and stimulants from hydroxyapatite nanoparticles functionalized with humic substances: toward a multifunctional Nanofertilizer. ACS Omega 5, 6598–6610.

Zahn, D., Hochrein, O., 2003. Computational study of interfaces between hydroxyapatite and water. Phys. Chem. Chem. Phys. 5, 4004–4007.
Zantua, M.I., Dumenil, L.C., Bremner, J.M., 1977. Relationships between soil urease activity and other soil properties. Soil Sci. Soc. Am. J. 41, 350–352.
Zettner, A., Sylvia, L.C., Capachodelgado, L., 1966. The determination of serum iron and iron-binding capacity by atomic absorption spectroscopy. Am. J. Clin. Pathol. 45, 533–540.
Zilversmit, D., Davis, A.K., 1950. Microdetermination of plasma phospholipids by trichloroacetic acid precipitation. J. Lab. Clin. Med. 35, 155–160.
Zook, E.G., Greene, F.E., Morris, E., 1970. Nutrient composition of selected wheats and wheat products. 6. Distribution of manganese, copper, nickel, zinc, magnesium, lead, tin, cadmium, chromium, and selenium as determined by atomic absorption spectroscopy and colorimetry. Cereal Chem. 47, 720–731.